ORIGINAL PAPER

# Luminescence and other spectroscopic properties of purple and green Cr-clinochlore

**Maria Czaja · Mariola Kądziołka-Gaweł · Radosław Lisiecki · Sabina Bodył-Gajowska · Zbigniew Mazurak**

**Abstract** For the first time ever, the luminescence spectra of $Cr^{3+}$ centers in two chlorite crystals are presented. Chromium ions occupy the strong crystal-field site M4 in the brucite sheet and the intermediate crystal-field site in the inner octahedral sheet for purple and green chlorite, respectively. We discuss the influence of an effective positive charge on the $Cr^{3+}$ ion and an effective negative charge of ligands on the differences in the values of the Dq and B parameters. It is concluded that the presence of $Fe^{2+}$ ions and other point defects, as well as concentration quenching, causes the very short luminescence lifetimes of chromium ions.

**Keywords** Cr-clinochlore · Luminescence · Optical absorption · Infrared · Raman and Mössbauer spectra

M. Czaja (✉) · S. Bodył-Gajowska
Faculty of Earth Sciences, University of Silesia, Będzińska 60, 41-200 Sosnowiec, Poland
e-mail: maria.czaja@us.edu.pl

M. Kądziołka-Gaweł
Faculty of Mathematics, Physics and Chemistry, University of Silesia, Uniwersytecka 4, 40-007 Katowice, Poland

R. Lisiecki
Institute of Low Temperature and Structure Research, Polish Academy of Sciences, Okólna 2, 50-422 Wrocław, Poland

Z. Mazurak
Center of Polymer and Carbon Materials, Polish Academy of Sciences, ul. M. Skłodowskiej-Curie 34, 41-819 Zabrze, Poland

## Introduction

The crystal structure refinement of Cr-chlorite was done by Phillips et al. (1980) as a consequence of earlier articles (Bailey and Brown 1962, Brown and Bailey 1963, Lister and Bailey 1967). Phillips et al. (1980) proposed discarding the names "kotschubeite" and "kämererite" as well as the use of the prefix "chromian" for Mg and other chlorites. They also definitely rejected the idea that $Cr^{3+}$ ions could be presented in a tetrahedral coordination. Several papers (Phillips et al. 1980, Zheng and Bailey 1989) have since shown that all Cr-chlorites are triclinic II$b$-4. In chlorite's structure, there are four octahedral positions for $Mg^{2+}$, $Al^{3+}$ and other ions, such as $Fe^{2+}$, $Fe^{3+}$, $Cr^{3+}$, $Mn^{2+}$ or $Ni^{2+}$. The M1 and M2 positions are localized in a talc-type layer, but M3 and M4 are in the brucite sheet. The average M1-(O,OH), M2-(O,OH), and M3-OH distances for Cr-clinochlore are about 0.207 nm, and for M4-OH, it is 0.1963 nm (Phillips et al. 1980, Zheng and Bailey 1989). In the purple chlorite specimens studied by Phillips et al. (1980), the $Cr^{3+}$ ions preferred the M4 octahedral site in a brucite sheet, contrary to the suppositions of Zheng and Bailey (1989), who proposed, with regard to their green color similar to fuchsite, that chromium ions are present in an inner octahedral sheet in site M1 or M2. The $Cr_2O_3$ contents of ten chlorite specimens studied by Phillips et al. (1980) varied from 1.52 to 8.31 weight percent (wt%), and in chlorite studied by Zheng and Bailey (1989) they were equal to 1.68 wt%.

Cr-chlorite specimens have not been adequately studied with spectroscopic methods. Many papers show the changes occurring in the Raman and IR spectra as a function of Si → Al and Fe → Mg substitutions. The increase of $Me^{3+}$ → $Si^{4+}$ substitution causes the frequency of the fundamental Si–O vibration to decrease; however, the

number of Si–O vibrations do not increase. For a higher amount of $Al^{3+}$ in tetrahedral coordination, the $Si^{IV}$–O and $Al^{IV}$–O bands overlap at about 990 $cm^{-1}$. Some correlation between vibrational bands and the chemical composition of Cr-chlorites was determined from the IR spectra by Tuddenham and Lyon (1959), and from a micro-Raman study by Prieto et al (2003). For crystals of a purple Cr-chlorite from Erzerum (Turkey), it was found that the frequency of the peaks at 681 and 199 $cm^{-1}$ strongly depended on (Fe, Al, Cr) → Mg substitution (Prieto et al. 2003). The Cr-clinochlores are distinguished by vibrations at 822/811 and 655/647 $cm^{-1}$ (Tuddenham and Lyon 1959). The effects of substituting central cations from the octahedral sheet of the trioctahedral phyllosilicates on the inner hydroxyl group was studied by Scholtzová et al (2003). Replacement of Si by Al results in a negative charge on oxygen, which is directly coordinated to the Al; and as a consequence, a distortion of the lattice occurs and a broadening of the OH stretching absorption is observed. The vibrations of the $Mg_3(OH)_6$ and of the medium intense band at 669 $cm^{-1}$ are shifted to lower frequencies when Mg is substituted by Al, Fe and other atoms. The frequencies of OH-Me vibrations of the brucite sheet is lower than those in the inner octahedral sheet, often at 3,580 $cm^{-1}$–3,450 $cm^{-1}$ (Farmer 1974). Shirozu's studies of Raman spectra (1980, 1985) have shown that vibrations of hydrogen bonding (SiSi)O….OH and (SiAl)O….OH take place. The substitution of Al → Si and Fe (or other ion) → Mg induced shifts of these bands to a lower frequency.

Based on Mössbauer spectra, it has been demonstrated that $Fe^{2+}$ ions are present in M1 and M2 crystal sites, and $Fe^{3+}$ ions are present in M3 and M4 crystal sites, as well as in a tetrahedral coordination (Goodman and Bain 1979, Blaauw et al. 1980, Dyar 1987, deGrave et al. 1987, Gregori and Mercader 1994, Smyth et al. 1997). The influence of $Al^{3+}$ → $Si^{4+}$ substitution, as well as of the Fe/Mg ratio on spectroscopic parameters of iron ions has been discussed in many papers (Annersten 1974, Dyar 1987, Gregori and Mercader 1994). The presence of $Fe^{2+}$ in tetrahedral sheet is mentioned by Gregori and Mercader (1994) because of the unusually low quadrupole splitting (QS) equal to 0.76 mm/s, and the rather large isomer shift (IS) value of 1.06 mm/s.

Bish (1977) presented the optical absorption spectra of ten Cr-chlorite specimens. Observed differences in their absorption spectra and those of the Cr- muscovite (fuchsite) led him to conclude that Cr ions should be present in an interlayer octahedral sheet. The color of the chlorite specimens studied in this paper cannot be clearly seen, however, it could be concluded from the absorption spectra that all of them were red or purple. For almost all of these chlorite specimens, the crystal field splitting parameter was above 1,800 $cm^{-1}$ and parameter B Racaha was less than 800 $cm^{-1}$. The absorption spectrum of chlorite from Erzerum (Turkey), measured in a VIS spectral range, which consists of $Cr^{3+}$ and $Fe^{2+}$ bands, has also been presented by Prieto et al (2003). To the best of our knowledge, no green Cr-clinochlore has been studied thus far, even though on the Internet, some collectors have published photographs of green chlorite from chromite deposits or samples occurring together with uvarovite—for example, the brilliant Cr-clinochlore from the Saranovskii Mine in the Middle Urals (http://www.mindat.org/locdetailed-2807.html).

The only luminescence spectra of Cr-chlorite published were in Czaja (1999) and Czaja (2002). The luminescence of the $Cr^{3+}$ ion can originate from $^2E_g \rightarrow {}^4A_{2g}$ or $^4T_{2g} \rightarrow {}^4A_{2g}$ transitions for strong and weak crystal fields, respectively, and from both of these two transitions simultaneously at room temperature when the crystal field is intermediate. Sharp emission lines $R_1$, $R_2$ and broad emission bands can be measured, sometimes with ZPL at low temperature and vibronic sidebands. However, additional luminescence lines sometimes appear at longer wavelengths in relation to the R lines. Some additional lines have been studied for synthetic materials with a significant content of $Cr_2O_3$ (Imbush 1967, Powell et al. 1967, Szymczak et al. 1975, Dereń et al. 1996). For natural topaz crystals, the contents of various amounts of the Cr, Mn and V have been shown as well (Gaft et al. 2003). These lines originate on near-neighbor pairs of chromium ions, where the ions forming the pair are strongly exchange-coupled and are usually called "$N_i$-lines". Energy transfer from isolated $Cr^{3+}$ ions to pairs of Cr–Cr can be observed. Imbush (1967) showed for $Al_2O_3$ doped with 0.003–1.0 atomic percent (at.%) of chromium that the intensity of N-lines at 77 K was almost equal to the intensity of the $R_1$ line. Powell et al. (1967) showed that at low temperature the intensity of N lines is higher than that of R lines, even for 0.94 wt% $Cr_2O_3$, and, of course, the same is true for greater chromium amounts. The decay times of R and N lines are very similar (several milliseconds), however, some differences in the decay rate at a low temperature have been noticed.

Some of the additional lines in emission spectra can be attributed to non-equivalent $Cr^{3+}$ centers, which are characterized by different ligands surrounding topaz crystals (Tarashchan et al. 2006), or to differences in next-nearest coordination (Walker et al. 1997). These lines are mentioned as emission lines originating from the $^2E_g$ level of $Cr^{3+}$ ions residing in distinct crystal sites. The energies (or wavelengths) of such lines and their intensities depend on the energy of excitation, which should be characteristic for each individual emission center. On the other hand, the effect of temperature on emission properties and lifetimes of excited states has not been discussed.

**Table 1** The chemical composition of the studied chlorite crystals

| wt% | Purple chlorite Part I | Purple chlorite Part II | Green chlorite |
|---|---|---|---|
| $SiO_2$ | $33.369 \pm 0.009$ | $28.713 \pm 0.008$ | $26.327 \pm 0.008$ |
| $TiO_2$ | $0.014 \pm 0.012$ | $0.0011 \pm 0.012$ | $0.0186 \pm 0.012$ |
| $Al_2O_3$ | $11.806 \pm 0.003$ | $23.027 \pm 0.003$ | $25.771 \pm 0.003$ |
| $Cr_2O_3$ | $4.262 \pm 0.122$ | $0.532 \pm 0.015$ | $1.929 \pm 0.055$ |
| $MgO$ | $34.844 \pm 0.007$ | $32.349 \pm 0.007$ | $31.254 \pm 0.007$ |
| $CaO$ | $0.041 \pm 0.001$ | $0.0073 \pm 0.001$ | $0.007 \pm 0.001$ |
| $MnO$ | $0.041 \pm 0.001$ | $0.028 \pm 0.001$ | $0.021 \pm 0.001$ |
| $FeO$ | $2.247 \pm 0.01$ | $1.610 \pm 0.01$ | $1.040 \pm 0.01$ |
| $Na_2O$ | n.d. | n.d. | 0.01 |
| $K_2O$ | $0.011 \pm 0.001$ | n.d. | $0.007 \pm 0.001$ |
| $H_2O$ | 13.407 | 12.711 | 12.681 |
| Total | 100.042 | 98.979 | 99.066 |
| Formulas recalculated to 36 oxygen atoms | | | |
| Si | 6.320 | 5.316 | 4.976 |
| Ti | 0.001 | 0.000 | 0.003 |
| Al | 2.468 | 5.024 | 5.738 |
| Cr | 0.636 | 0.078 | 0.288 |
| Mg | 9.838 | 8.928 | 8.802 |
| Ca | 0.001 | 0.001 | 0.001 |
| Mn | 0.003 | 0.004 | 0.001 |
| $Fe^{3+}$ | 0.074 | 0.074 | 0.078 |
| $Fe^{2+}$ | 0.104 | 0.103 | 0.086 |
| Na | 0.000 | 0.000 | 0.003 |
| K | 0.007 | 0.000 | 0.001 |
| Fe/Mg | 0.032 | 0.028 | 0.018 |
| $Fe^{2+}/Fe^{3+}$ | 1.36 | 1.38 | 1.102 |
| $Na^+K^{+2}Ca$ | 0.010 | 0.003 | 0.008 |

The luminescence of purple chlorite is rather unusual because of a quite high amount of $Cr_2O_3$ in this crystal. Accordingly, effective concentration quenching of luminescence might be expected. Indeed, the emission of $Cr^{3+}$ ions is rather weak at room temperature but grows markedly when temperature decreases. Moreover, the $R_1$ line is accompanied by other bands at the lower energy range of the spectrum. An additional line appears on the emission spectra of green chlorite as well. The origin of these bands and lines, as well as their luminescence decay times need to be explained. The luminescence properties of these crystals are interesting and can expand our knowledge on the luminescence properties of $Cr^{3+}$ ions in natural crystals.

Sample properties and measurement conditions

The purple Cr-clinochlore studied here was found in Kop ophiolitic ultramafic rocks from the Erzincan deposit (Turkey). Our specimen is reddish-purple, with purple-to-pink pleochroism, a vitreous luster, and a perfect cleavage

with a (001) plane, formed as an aggregate of several pseudohexagonal and clear single crystals up to 150 μm thick. This chlorite was found in incrustations on the walls of vugs and cracks in a serpentinized basic rock. According to a chemical analysis by Brown and Bailey (1963), this chlorite has the following composition: $(Si_3Al)(Mg_5Fe_{0.1}^{2+}Cr_{0.7}Al_{0.2})(O_{18}H_{7.9})$. Such chlorite varieties are commonly called "kämmererite". The $Cr_2O_3$ content in the chlorite specimens is nearly 6 wt% for this deposit (Andrut et al. 1995). The green chromian clinochrore is from the Sludorudnik Mine (South Ural, near Kysztym). The crystals are deep-green, with a distinct green-to-colorless pleochroism, a vitreous luster, and a perfect cleavage with (001) plane, formed as an aggregate of several pseudo-hexagonal and clear, single crystals up to 250 μm thick.

The chemical composition of the studied chlorite specimens was determined using an electron-microprobe analyzer (CAMECA sx100; 15 kV, 40–50 nA). The following lines and standards were used: $CaK\alpha$, $SiK\alpha$, $MgK\alpha$ (diopside), $TiK\alpha$ (rutile), $CrK\alpha$ ($Cr_2O_3$), $AlK\alpha$ (orthoclase), $FeK\alpha$ ($Fe_2O_3$), $MnK\alpha$ (rhodochrosite). Corrections were made using a PAP procedure provided by CAMECA. The results are presented in Table 1.

Mössbauer spectra were measured using a constant acceleration spectrometer with a $^{57}Co:Cr$ source. All measurements were carried out at room temperature. The velocity calibration of the spectrometer was done with an α-Fe metallic powder absorber. The isomer shift (IS) is given in relation to $Is_{\alpha-Fe}$. The obtained spectra were fitted as a superposition of several doublets. The decomposition into doublets was performed by Lorentzian function. The results are shown in Fig. 1a, b and Table 2.

Unpolarized FTIR and Raman spectra were obtained with a Bio-Rad FTS-6000 spectrometer with a micro-ATR accessory. They are presented in Fig. 2a, b, and the frequencies of IR and R bands are listed in Table 3.

Polarized absorption spectra of purple and green chlorite crystals were measured at room temperature using a Cary-Varian Model 2300 spectrophotometer in the spectral range from 2,000 nm (5,000 cm$^{-1}$) to 340 nm (30,000 cm$^{-1}$) and are presented in Fig. 3a, b. There were two idiomorphic slabs oriented in parallel to the (001) plane, so the spectra nearly in parallel to the X and Y axis were measured.

The steady time-luminescence spectra of the chlorites studied herein were performed using a Jobin–Yvon (SPEX) spectrofluorimeter FLUORLOG 3-12 at room temperature with a 450W xenon lamp, a double-grating monochromator, and a Hamamatsu 928 photomultiplier. The measurements at low temperatures up to 15 K were made using a Physik LPD3000 laser (pumped by a Lambda Physik LPX100 excimer laser). The emission spectra are presented in Fig. 4a, b. Luminescence decay curves were measured upon a pulsed excitation delivered by a Continuum Surelite

**Table 2** Mössbauer doublet assignments for purple and green chlorite crystals

| Samples doublets | | IS (mm s$^{-1}$) | QS (mm s$^{-1}$) | A (%) |
|---|---|---|---|---|
| Purple chlorite | D1—Fe$^{2+}$ in M1 (trans) site | 1.109 ± 0.014 | 2.528 ± 0.030 | 26.1 |
| | D2—Fe$^{2+}$ in M2 (cis) site | 1.125 ± 0.002 | 2.768 ± 0.010 | 27.0 |
| | D3—Fe$^{3+}$ in tetrahedral sheet | 0.103 ± 0.019 | 0.506 ± 0.036 | 33.2 |
| | D4—Fe$^{3+}$ in M4 site (brucite sheet) | 0.338 ± 0.017 | 0.690 ± 0.036 | 4.6 |
| | D5—(Fe$^{2+}$+Fe$^{3+}$) or Fe$^{2.5+}$ in M3 and M4 sites | 0.560 ± 0.110 | 1.394 ± 0.018 | 9.1 |
| Green chlorite | D1—Fe$^{2+}$ in M1 (trans) site | 1.075 ± 0.013 | 2.136 ± 0.026 | 7.2 |
| | D2—Fe$^{2+}$ in M2 (cis) site | 1.127 ± 0.004 | 2.630 ± 0.010 | 45.3 |
| | D3—Fe$^{3+}$ in tetrahedral sheet | 0.119 ± 0.007 | 0.454 ± 0.012 | 47.5 |

**Table 3** Position of the infrared and Raman bands of the studied chlorite crystals

| Position of vibration bands (cm$^{-1}$) | | | | Assignment |
|---|---|---|---|---|
| FTIR purple chlorite | FTIR green chlorite | Raman purple chlorite | Raman green chlorite | |
| 3,677 | 3,663 | | | ν(OH) of talc-type layer |
| 3,580 | 3,567 | | | IR spectra: ν(OH) Mg$_2$AlOH of brucite sheet (SiSi)O….OH and (SiAl)O….OH |
| 3,435 | 3,442 | | | |
| 1,086 | | | | ν(T$_4$O$_{10}$) stretching, mainly S–O–Si |
| 1,056 | | | | |
| 996s | 985 s | | | |
| 958s | | | | |
| | 891 w | | | ? |
| 821 w | 831 m | | | Al$^{IV}$–O |
| 771 w | 771 m | | | (Si,Al)–O–OH libration |
| | | 682 s | | Mg–O–OH of inner octahedral sheet |
| | | | 668 s | (Mg,Cr)–O–OH of inner octahedral sheet |
| | 670 s | | | Mg(OH)$_6$ of brucite sheet |
| 648 s | | | | (Mg,Cr)(OH)$_6$ of brucite sheet |
| – | – | – | 610 w | ? |
| 525 m | 538 m | 541 | 551 | δ (T$_4$O$_{10}$) bending, mainly Si–O–Si |
| 459 s | 467 s | – | – | δ (T$_4$O$_{10}$) bending, mainly Si–O–Si |
| 442 s | 444 s | 458 m | 446 s | |
| 417 s | – | – | – | |
| | | 355 m | 359 m | (Me-O-OH) of talc-like layer |
| | | 311–282 w | 276 w | δ (T$_4$O$_{10}$) bending, mainly Si–O–Si |
| | | 238 w | – | ? |
| | | 198 s | 214 s | Me(OH)$_6$ of brucite sheet |

optical parametric oscillator (OPO) pumped with the third harmonic of an Nd:YAG laser. The decays were measured with a Hamamatsu R-955 photomultiplier connected to a Tektronix Model TDS 3052 digital oscilloscope.

## Results and discussion

The composition of the purple chlorite (Table 1) is chemically variable and inhomogeneous. Moreover, there are

some zones rich in Cr. The Pearson correlation coefficients were calculated. The Si content is clearly anti-correlated with Al (−0.994) and strongly correlated with Mg (+0.998) and Cr (+0.985). It is rather distinct in its relation to Fe (+0.831). Furthermore, the relations of Al content to Cr, Mg or Fe contents are changeable, which means they are anti-correlated (−0.993, −0.987 and −0.795, respectively). In this Cr-chlorite, there are zones rich in Si, Mg, Cr and less rich in Fe. Al content increases, and the content of Cr decreases, within zones with a lower concentration of Si.
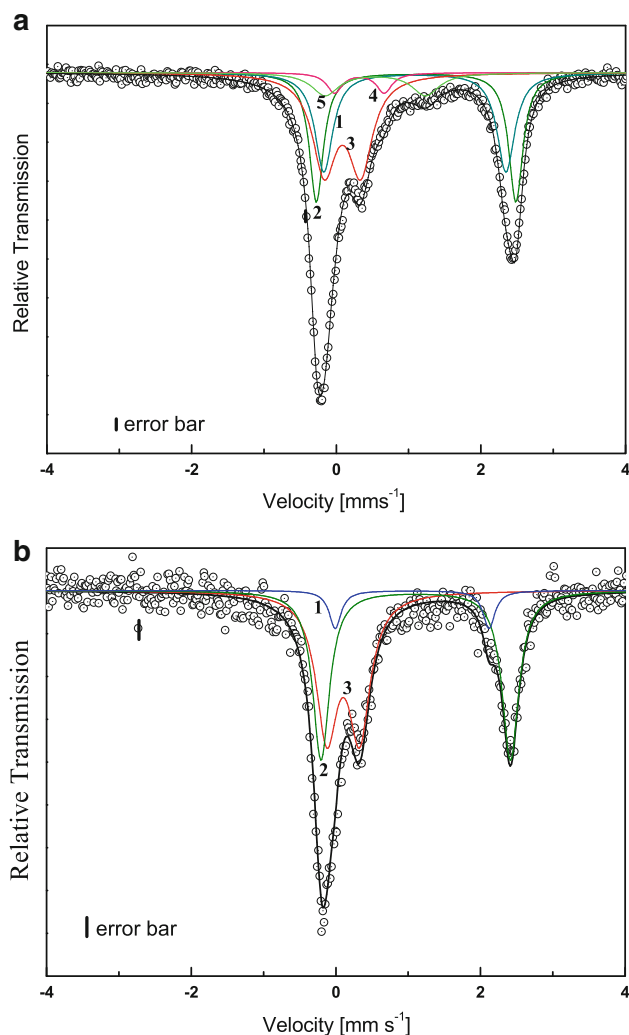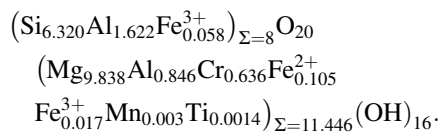
Fig. 1 a The Mössbauer spectrum of purple chlorite. The *numbers* indicate the doublets, according to Table 2. b The Mössbauer spectrum of green chlorite. The *numbers* indicate the doublets, according to Table 2

The chemical composition of the green chlorite is practically homogeneous. Only the content of Ti is substantially variable. This specimen looks very similar to the green chlorite from Kenya studied earlier by Steinfink (1958) and Bailey (1975), and our results are comparable to theirs. The green chlorite has higher $Al^{IV}$ content in contrast to that of our purple chlorite and that other chlorites studied by Phillips et al (1980).
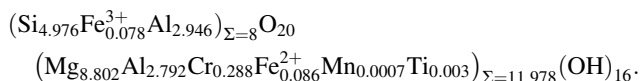
The Mössbauer spectra of the studied chlorite crystals presented in Fig. 1a, b show that both $Fe^{3+}$ and $Fe^{2+}$ ions are present in our samples. The content of iron in the M1–M4 sites has been calculated and is presented herein in Table 2. $Fe^{3+}$ in both studied crystals occurs in tetrahedral sites, but in purple chlorite it is also present in the octahedral sheet. Doublet D4 has IS and QS parameters that are characteristic of the M4 site (Smyth et al. 1997). On the

MS of the purple chlorite, yet another doublet D5 has been identified, and its parameters are characteristic for neither $Fe^{2+}$ nor $Fe^{3+}$ ions. Doublets with $0.5 > IS > 0.9$ mm s$^{-1}$ are generally understood to represent delocalization of electrons between adjacent $Fe^{3+}$ and $Fe^{2+}$, resulting in an average value of IS that can be assigned to $Fe^{2.5+}$ (Dyar et al. 2006). It is reasonable to assume that $Fe^{2+}$–$Fe^{3+}$ ions are present in the M3 and M4 sites in the brucite sheet. The authors assume that half of these ions are $Fe^{2+}$ and half are $Fe^{3+}$. In Table 1, the number of all cations, including $Fe^{2+}$ and $Fe^{3+}$ was computed into a proper per unit formula. The $Fe^{2+}/Fe^{3+}$ ratio is equal to 1.36 and 1.10 for purple and green chlorite, respectively. The higher amount of $Fe^{3+}$ ions that reside in the tetrahedral site of green chlorite results from a smaller amount of Si. Because for $Fe^{2+}$ (the reverse of $Fe^{3+}$) a lower quadrupole splitting means more distortion around a site, the measured doublets D1 were ascribed as originating from the M1 site. However, the majority of ferrous ions occupy M2 sites in purple and green Cr-clinochlore. In fact, the symmetry of sites M1 and M2 in purple Cr-clinochlore seems to be more regular than in the green specimen. Differences in the electric field gradient for green chlorite may be caused by $Cr^{3+}$ ions in the M1 or M2 sites that are located in the inner octahedral sheet, as is observed for fuchsite. The different IS parameter values for the M1 site in the purple and green chlorite crystals could be said to be a consequence of the higher Al amount in the tetrahedral sheet and various Fe/Mg ratios for the green chlorite sample, which is in line with the results reported previously (Annersten 1974, Dyar 1987, Gregori and Mercader 1994).

The chemical formula of the studied Cr-purple clinochlore in the first approximation is the following:

$$\left(Si_{6.320}Al_{1.622}Fe^{3+}_{0.058}\right)_{\Sigma=8}O_{20}$$
$$\left(Mg_{9.838}Al_{0.846}Cr_{0.636}Fe^{2+}_{0.105}\right.$$
$$\left.Fe^{3+}_{0.017}Mn_{0.003}Ti_{0.0014}\right)_{\Sigma=11.446}(OH)_{16}.$$

The deficiency of the occupation of cation sites and positive charges ($-1.28$, i.e. 2.2 %) should not be neglected. The chemical composition of the green Cr-clinochlore crystal is as follows:

$$\left(Si_{4.976}Fe^{3+}_{0.078}Al_{2.946}\right)_{\Sigma=8}O_{20}$$
$$\left(Mg_{8.802}Al_{2.792}Cr_{0.288}Fe^{2+}_{0.086}Mn_{0.0007}Ti_{0.003}\right)_{\Sigma=11.978}(OH)_{16}.$$

For this sample, the deficiency of the positive charge is insignificant, namely, $+0.022$ (i.e. 0.04 %).

The infrared and Raman spectra of these crystals are shown in Fig. 2a, b. Appropriate vibration modes (Table 3) were assigned according to Tuddenham and Lyon (1959), Stubican and Roy (1961), Farmer (1974), Shirozu and Ishida (1982), and Prieto et al (1991). Three intensive
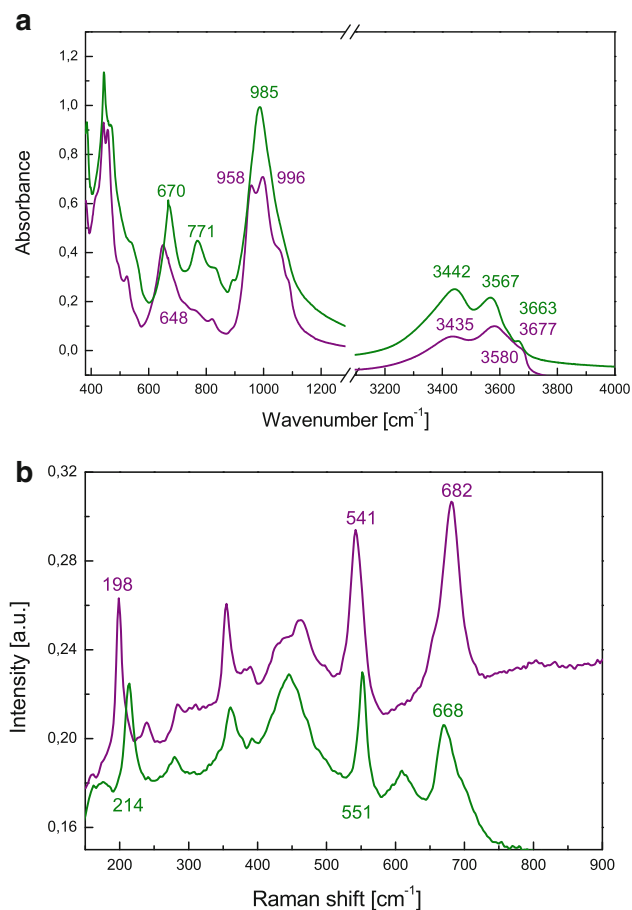
**a**



**b**



Fig. 2 **a** The infrared spectra of studied chlorite crystals. The *purple line* for purple chlorite, the *olive line* for green chlorite. **b** The Raman spectra of studied chlorite crystals. The *purple line* for purple chlorite, the *olive line* for green chlorite
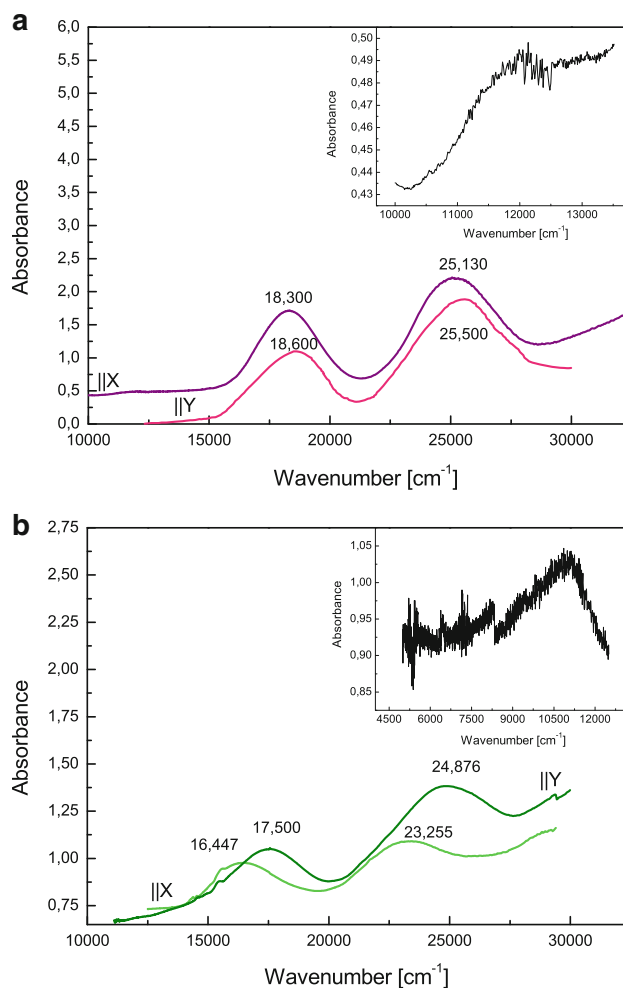
**a**



**b**



Fig. 3 **a** The polarized absorption spectra of $Cr^{3+}$ ion in purple chlorite. The *purple line* is for E∥X and the pink line is for E∥Y. Inset: the absorption spectrum of $Fe^{2+}$ ion in purple chlorite. **b** The polarized absorption spectra of $Cr^{3+}$ ion in green chlorite. The *olive line* is for E∥Y and the green line is for E∥X. Inset: the absorption spectrum of $Fe^{2+}$ ion in green chlorite

bands can be observed in the FTIR spectra within 3,700–3,000 cm$^{-1}$. The band with the highest frequency is related to ν(OH) of the 2:1 layer. For the green crystal, this band is located at a lower frequency (3,665 cm$^{-1}$) than the one at which it is observed (3,670 cm$^{-1}$) for the purple crystal. Accordingly, we can conclude that the inner octahedral sheet of green chlorite contains more heavy atoms in comparison to the purple chlorite. For the green chlorite, the next band appears at a lower frequency (3,568 cm$^{-1}$) than for the purple chlorite (3,582 cm$^{-1}$). It can be concluded that the higher number of $Al^{3+}$ ions occupies the tetrahedral sheet in the green chlorite. For the purple chlorite crystal, the next band occurs at a lower frequency (3,434 cm$^{-1}$) than is recorded for the green chlorite (3,442 cm$^{-1}$). It indicates that $Mg^{2+}$ ions in the brucite sheet are substituted by heavy ions in greater quantities than in the green chlorite. The substantial amount of $Al^{3+}$ ions in the tetrahedral sheet of the green chlorite causes the Si–O stretching band placed at 1,080–1,000 cm$^{-1}$ to be unresolved and shifted towards a lower frequency, in

relation to the same band observed in the purple crystal. Considerable differences in IR and Raman spectra are related to bands below 700 and near 200 cm$^{-1}$, which are in turn related to the brucite Me-OH libration. It has already been demonstrated that for purple chlorite, the heavy ions in the $Me(OH)_6$ sheet cause a shift of the bands to a lower frequency in comparison to the same bands recorded for the green chlorite sample. In fact, the main differences noticed in the FTIR and Raman spectra of the chlorites studied in this paper are caused by a large amount of chromium in the brucite sheet (the purple chlorite) that is charge-balanced by $Al^{3+}$ ions in the tetrahedral sheet (the green chlorite).

Absorption spectra recorded in the VIS–NIR spectral range are presented in Fig. 3a, b. The $^5T_{2g} \rightarrow {}^5E_g$ transitions of $Fe^{2+}$ can be observed at 11,760 cm$^{-1}$ and

**Table 4** Spectroscopic parameters of $Cr^{3+}$ and $Fe^{2+}$ ions in the studied chlorite crystals

| | The spectroscopic parameters of the $Cr^{3+}$ ion | | | | | The spectroscopic parameters of the $Fe^{2+}$ ion | | |
| --- | --- | --- | --- | --- | --- | --- | --- | --- |
| | Dq (cm$^{-1}$) | B (cm$^{-1}$) | Dq/B | CSFE (kJ/mol) | CSFE (kcal/mol) | Dq (cm$^{-1}$) | CFSE (kJ/mol) | CSFE (kcal/mol) |
| Purple chlorite (‖X) | 1,830 | 669 | 2.74 | 262.3 | 62.8 | 1,176 | 56.2 | 13.5 |
| Purple chlorite (‖Y) | 1,860 | 674 | 2.75 | 266.6 | 63.8 | | | |
| Green chlorite (‖X) | 1,645 | 704 | 2.34 | 235.8 | 56.5 | 1,098 | 52.5 | 12.5 |
| Green chlorite (‖Y) | 1,750 | 744 | 2.35 | 250.8 | 60.1 | | | |

10,975 cm$^{-1}$ for the purple and green crystals, respectively. The different energy levels of these bands indicate that the crystal field splitting of $Fe^{2+}$ ions occupying the M1 and M2 sites in the purple chlorite is higher than in the green crystal. The main reason for this could be traced to a slightly longer Fe–O distance in the green chlorite relative to red chlorite. The trivalent $Cr^{3+}$ ions are present in the inner octahedral sheet in the green chlorite; thus, the enhancement of the repulsion between cations may be significant. The differences observed in the absorption spectra are clear, especially in the VIS spectral range. Two prominent absorption bands due to spin-allowed transitions of $Cr^{3+}$ ion in the octahedral environment are assigned to the following transitions:

For purple chlorite ${}^4A_{2g} \rightarrow {}^4T_{2g}$ at $18,300$ cm$^{-1}$ (‖X)

and $18,600$ cm$^{-1}$ (‖Y)

${}^4A_{2g} \rightarrow {}^4T_{1g}$ at $25,130$ cm$^{-1}$ (‖X)

and $25,500$ cm$^{-1}$ (‖Y).

For green chlorite ${}^4A_{2g} \rightarrow {}^4T_{2g}$ at $16,447$ cm$^{-1}$ (‖X)

and $17,500$ cm$^{-1}$ (‖Y)

${}^4A_{2g} \rightarrow {}^4T_{1g}$ at $23,255$ cm$^{-1}$ (‖X)

and $24,876$ cm$^{-1}$ (‖Y)

The parameters Dq, B Racaha, Dq/B, and CFSE are shown in Table 4.

Results obtained for the purple chlorite are similar to those obtained by Płatonow et al. (1995) and Andrut et al (1995). The Dq and Dq/B values indicate that in the purple chlorite crystals, $Cr^{3+}$ ions are influenced by a strong crystal field. To the best of our knowledge, the rate of Dq is the highest value reported to date for $Cr^{3+}$ ions in natural crystals and in synthetic materials. As a consequence, the crystal-field stabilization energy (CFSE) is the highest for Cr minerals. Moreover, the Racaha B parameter is low; thus, the nature of $Cr^{3+}$–$O^{2-}$ bonding is covalent-ionic. The purple color of this crystal is the result of mixing blue and red colors, which are not absorbed throughout the crystal. The influence of the strong crystal field on $Cr^{3+}$ ions supports our earlier supposition that these ions in the purple chlorite occupy the M4 site in the brucite sheet. The
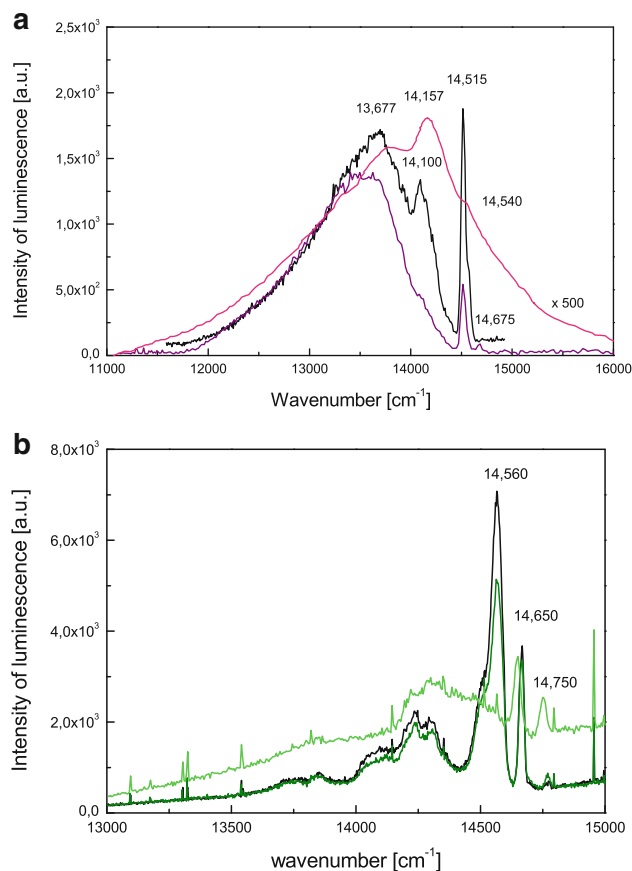


**Fig. 4 a** The luminescence spectra of the $Cr^{3+}$ ion in purple chlorite measured at different temperatures; the *pink line*—T = 300 K, the *purple line*—T = 77 K, the *black line*—T = 15 K. **b** The luminescence spectra of the $Cr^{3+}$ ion in green chlorite measured at different temperatures; the *green line*—T = 300 K, the *olive line*—T = 77 K, the *black line*—T = 20 K

polarized absorption spectra of this crystal showed a rather weak pleochroism: from purple for E‖X to pink for E‖Y.
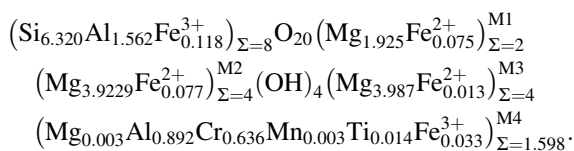
To the best of our knowledge, the absorption spectra of the green Cr-chlorite shown in Fig. 4b are documented herein for the first time. For the green chlorite, Dq and Dq/B values are characteristic of the intermediate crystal field, just as for Cr-beryl or Cr-vesuvianite. The polarized absorption spectra of this crystal feature pleochroism from blue-green for E‖X to green for E‖Y. The energies of

$^4A_{2g} \rightarrow {}^4T_{2g}$ and $^4A_{2g} \rightarrow {}^4T_{1g}$ transitions are considerably different for $Cr^{3+}$ ions occupying the low-symmetry site (or sites). Moreover, the Cr–O distance should be greater than for the M4 site. This means that $Cr^{3+}$ ions in the green chlorite do not occur in the brucite sheet but in the inner octahedral sheet, probably in the M2 or M1 site as was earlier assumed by Zheng and Bailey (1989) for the light green chlorite from Kenya, but without any evidence. Because the M2 site is less regular than the M1 site, it seems to be more appropriate for the chromium ion, but we do not have any structural evidence to support such an assumption at this time.
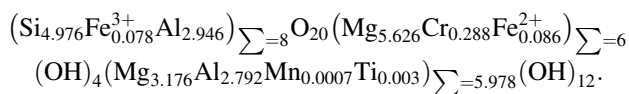
The characteristic dips seen on the absorption spectra of the green chlorite are evidence of the Fano antiresonant effect resulting from the interaction of the $^2T_{1g}(G)$ and $^2E_g(G)$ with a vibrationally broadened $^4T_{2g}(F)$ state. These dips are sharp because there is no change in the electronic configuration $(t_{2g}^3)$ for $^4A_{2g}$ and $^2T_{1g}(^2G)$ or $^2E_g(^2G)$ levels. This effect is often measured for Cr-doped glass (Stręk et al. 1983, Illaremandi et al. 1993). The positions of these bands are: 15,620 $cm^{-1}$ for the $^4A_{2g} \rightarrow {}^2T_{1g}(^2G)$ transition and 14,590 $cm^{-1}$ and 14,447 $cm^{-1}$ for the $^4A_{2g} \rightarrow {}^2E_g(^2G)$ transition.

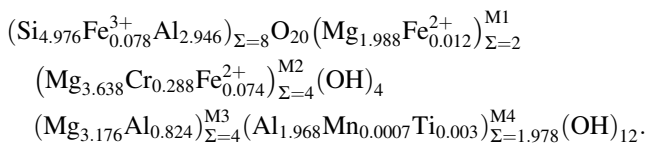Here, it is appropriate to propose the following chemical formulas:

(a) for the Cr-purple clinochlore (part I):

$$\left(Si_{6.320}Al_{1.562}Fe^{3+}_{0.118}\right)_{\Sigma=8} O_{20} \left(Mg_{1.925}Fe^{2+}_{0.075}\right)^{M1}_{\Sigma=2}$$
$$\left(Mg_{3.9229}Fe^{2+}_{0.077}\right)^{M2}_{\Sigma=4} (OH)_4 \left(Mg_{3.987}Fe^{2+}_{0.013}\right)^{M3}_{\Sigma=4}$$
$$\left(Mg_{0.003}Al_{0.892}Cr_{0.636}Mn_{0.003}Ti_{0.014}Fe^{3+}_{0.033}\right)^{M4}_{\Sigma=1.598}.$$

(b) for the green Cr-clinochlore crystal:

$$\left(Si_{4.976}Fe^{3+}_{0.078}Al_{2.946}\right)_{\sum=8} O_{20} \left(Mg_{5.626}Cr_{0.288}Fe^{2+}_{0.086}\right)_{\sum=6}$$
$$(OH)_4 \left(Mg_{3.176}Al_{2.792}Mn_{0.0007}Ti_{0.003}\right)_{\sum=5.978} (OH)_{12}.$$

If chromium ions occupy the M2 site, the following chemical formula can be proposed:

$$\left(Si_{4.976}Fe^{3+}_{0.078}Al_{2.946}\right)_{\Sigma=8} O_{20} \left(Mg_{1.988}Fe^{2+}_{0.012}\right)^{M1}_{\Sigma=2}$$
$$\left(Mg_{3.638}Cr_{0.288}Fe^{2+}_{0.074}\right)^{M2}_{\Sigma=4} (OH)_4$$
$$\left(Mg_{3.176}Al_{0.824}\right)^{M3}_{\Sigma=4} \left(Al_{1.968}Mn_{0.0007}Ti_{0.003}\right)^{M4}_{\Sigma=1.978} (OH)_{12}.$$

For the purple chlorite, a deficiency of negative charge is observed in the tetrahedral sheet and, consequently, for the talc-type layer this deficiency is equal to 0.32 (per 28 oxygen atoms formula), and the excess of negative charge in the brucite sheet equals 1.29. Consequently, the unit as a whole exerts an excess of negative charge equal to 0.97. This disequilibrium among the positive and negative

charges is caused by vacancies in the brucite sheet. It also means that the positive charge on cations in the brucite sheet is lower than for the ideal clinochlore crystal. When the effective positive charge on the 3d cation decreases, the Racaha parameter B decreases as well. Furthermore, as the effective negative charge on ligands of the brucite sheet is greater, the force of the crystal field increases. So the crystal-field parameters Dq and B of $Cr^{3+}$ ion in the M4 crystal site are determined not only by Cr–O distances but also by the chemical nature of all units. It is generally accepted that trioctahedral chlorites have a significant number of octahedral vacancies (Foster 1962, Morata et al. 2001). Foster (1962) stated that low octahedral totals are induced by the method of calculation and need not indicate the vacancies, and that octahedral totals <11.5 are common. The octahedral occupancy of the purple chlorite is substantially less than the ideal total of 12 cations for a fully trioctahedral chlorite. The low octahedral total results from higher $Al^{3+}$ in the tetrahedral rather than in the octahedral contents. For the purple chlorite, $\Sigma(R^{3+})^{IV} = 1.680$ and is higher than $\Sigma(R^{3+})^{VI} = 1.49$. This difference is equivalent to a 0.543 positive charge. The rest of the deficiency (0.737) can be explained by vacancies ranging from 0.03685 to 0.2456 of octahedral sites for 2+ and 3+ cations, respectively. The existence of vacancies in the purple chlorite is indirectly confirmed by an analysis of the green chlorite chemical and its unit formula, where $\Sigma(R^{3+})^{IV} = 3.024$ and $\Sigma(R^{3+})^{VI} = 3.080$, in which case the deficiency of the octahedral totals and the positive charge is negligible.

For the green chlorite, the talc-type layer has an excess of negative charge equal to 0.736 (caused by an 1.024 excess of the tetrahedral sheet minus an 0.288 excess of positive charge of the inner octahedral sheet), which is compensated by an excess of positive charge of the brucite sheet equaling 0.754. As is the case for the $Cr^{3+}$ ion in the inner octahedral sheet, the decrease of positive charge does not take place; it is not the cause of the decrease of the B Racaha parameter.

Płatonow et al. (1995) has put forward the thesis that the number and properties of next-neighbor cations in the octahedral and tetrahedral sheets ($Si^{4+}$, $Mg^{2+}$ and $Al^{3+}$) have the strongest effect on spectroscopic parameters Dq and B through the change of the effective charge of ligands surrounding the $Cr^{3+}$. However, in our opinion, there is no clear relation between the types of cations: $Si^{4+}$, $Mg^{2+}$ and $Al^{3+}$ as $Cr^{3+}$-neighbors and values of the B parameter. For example, $Mg^{2+}$ cations are the next-neighbor for $Cr^{3+}$ in Cr-diopside, Cr-grossular and knorringite, but the Racaha parameters are quite different (736 $cm^{-1}$, 670 $cm^{-1}$ and 640 $cm^{-1}$, respectively). In our two studied Cr-clinochlore crystals, it is primarily, if not exclusively, $Mg^{2+}$ ions that are present in the second coordination sphere, in the brucite sheet as well as in the talc-type layer.

$Cr^{3+}$ ions occupy the strong crystal field site in the purple chlorite and, consequently, an emission from the $^{2}E$ excited level should be expected. It was very hard to measure the emission of this crystal, especially at room temperature (Fig. 4a). The emission band at T = 300 K is broad, with peaks at 13,780, 14,157 and 14,540 cm$^{-1}$. When temperature decreases, the intensity of luminescence significantly increases. At T = 77 K, a sharp line at 14,515 cm$^{-1}$ appeared beside the intense band at 13,500 cm$^{-1}$, and at T = 15 K position of this band moved to 13,677 cm$^{-1}$ and an additional line has been located at 14,100 cm$^{-1}$. The emission line at 14,515 cm$^{-1}$ (15 K) could be recognized as the $R_1$ emission line associated with an $^{2}E_g \rightarrow {}^{4}A_{2g}$ transition. At room temperature, this emission was weak; it is possible that it is a shoulder at 14,540 cm$^{-1}$ (spectrum at 300 K). At temperature T = 77 K, a broad and intensive band at 13,500 cm$^{-1}$ is still present beside the $R_1$ line. This emission cannot correspond to the $^{4}T_{2g} \rightarrow {}^{4}A_{2g}$ transition. The is because in a strong crystal field the higher $^{4}T_{2g}$ excited level could not be populated at 77 K, since $\Delta E_q = E(^{4}T_{2g})-E(^{2}E_g)$ is above 1,000 cm$^{-1}$. Similarly, the sharp band at 14,100 cm$^{-1}$ (T = 15 K) cannot be recognized as a ZPL (zero-phonon line) from the $^{4}T_{2g}$ level. Neither the 14,100 cm$^{-1}$ line nor the 13,500 cm$^{-1}$ band can be recognized as an emission of $Fe^{3+}$ ions in a tetrahedral site, because the excitation spectra from them are, without doubt, characteristic for the $Cr^{3+}$ ion. The emission of $Mn^{2+}$ ions does not occur, either. It means that these two bands should be mentioned as luminescence from centers other than a single $Cr^{3+}$ ion in the M4 site. The distribution of $Cr^{3+}$ ions in the purple chlorite crystal is irregular, and fewer than one per ten sites in the brucite sheet are occupied by chromium ions. Therefore, it is possible to assume that in the purple chlorite, some clusters of $Cr^{3+}$ ions as well as Cr–Cr pairs may be present. For $Al_2O_3$ Cr- heavy doped up to 5 wt%, Barthem et al. (1982) measured R and N lines as well as the broad emission band at 771 nm (12,970 cm$^{-1}$). They linked this band to Cr clusters. The decay times of all emission lines measured at T = 77 K were distinctly shorter than those obtained by Powell et al. (1967) or Imbush (1967); the decay curves had a double-exponential character, and lifetimes amounted to 390 and 80 μs for a 3 wt% sample (Barthem et al. 1982). Therefore, it is possible to extrapolate on these premises that the emission band at 13,500 cm$^{-1}$ originated from Cr clusters. Therefore, the sharp emission band at 14,100 cm$^{-1}$ cannot also originate from the Cr–Cr pair, because an oversized difference of energy for the $R_1$ line (14,515 cm$^{-1}$) and mentioned band (415 cm$^{-1}$) is observed. Moreover, this line is absent at T = 77 K and appears only when T < 40 K. However, this luminescent center is associated with $Cr^{3+}$ ions and this may be due to $Cr^{3+}$ residing in defect sites, which are caused by adjacent point defects, most probably by vacancies in the brucite sheet. This effect is comparable to the results related to the emission lines measured by Walker et al. (1997) for $Cr^{3+}$ near other lattice point defects. The luminescence lifetimes of these lines were measured and are unusually short compared to the lifetimes of $Cr^{3+}$ luminescence in a strong crystal field (Fig. 5a). The decay curves have a double-exponential character even at low temperatures. The short luminescence lifetime could be caused by: (a) lattice phonon interaction; however this factor may be neglected for low temperature measurements, (b) concentration quenching, and (c) energy transfer to other active luminescence centers. Due to the last cause, the $Cr^{3+}$ to $Fe^{2+}$ energy transfer is most important. As the temperature is lowered to 120 K (160 K) the decay times increase; however, from 120 K (80 K) to 20 K they diminish again. The reduction of luminescence lifetime is caused by energy transfer to a new center that has been activated ($Cr^{3+}$ with vacancies—14,100 cm$^{-1}$ line). The double-exponential character of the decay curves can be attributed to two decay mechanisms, namely, concentration quenching and energy transfer to the clusters or $Cr^{3+}$ ions in defected crystal sites.

For the green chlorite, $Cr^{3+}$ ions occupy an intermediate crystal field site and their luminescence spectrum at room temperature is similar to alexandrite or beryl spectra. The emission spectrum measured at room temperature contains the $R_1$ (14,650 cm$^{-1}$) and $R_2$ (14,750 cm$^{-1}$) lines and the broad band centered at 14,315 cm$^{-1}$. When the temperature is lowered from 120 to 10 K, the additional sharp line at 14,560 cm$^{-1}$ appears and at low temperatures this line displays a higher intensity than the $R_1$ line (Fig. 4b). This additional line cannot be recognized as a ZPL (zero-phonon line) from the $^{4}T_{2g}$ or $^{2}E_g$ levels. The sole reasonable explanation is that this line at 14,560 originates from another luminescence center related to $Cr^{3+}$ ions or from Cr–Cr pairs. This additional line (14,560 cm$^{-1}$) can be recognized as an N line of Cr–Cr pairs. The following facts support this assumption:

(a)  from 105 K to 20 K, the intensity of this emission (N line) increases and the relative intensity of $R_1$ and N lines changes similarly to the results documented by Powell et al. (1967) (Fig. 5b);

(b)  experimental data of $I(R_1)/I(N)$ can be fitted at high temperatures to an exponential $e^{-\Delta E/kT}$, where $\Delta E$ is the difference in the energy of initial (metastable) levels of the two transitions involved, similar to the study by Powell et al. (1967); $\Delta E = 45$ cm$^{-1}$. The deviation from thermalization occurs at 65 K. Powell observed the thermalization for 2,1 at.% Cr in $Al_2O_3$ almost at the same temperature. In the green chlorite at.% Cr is equal to 2.4;

(c)  the $R_1$ emission line excites the N line at 14,560 cm$^{-1}$;
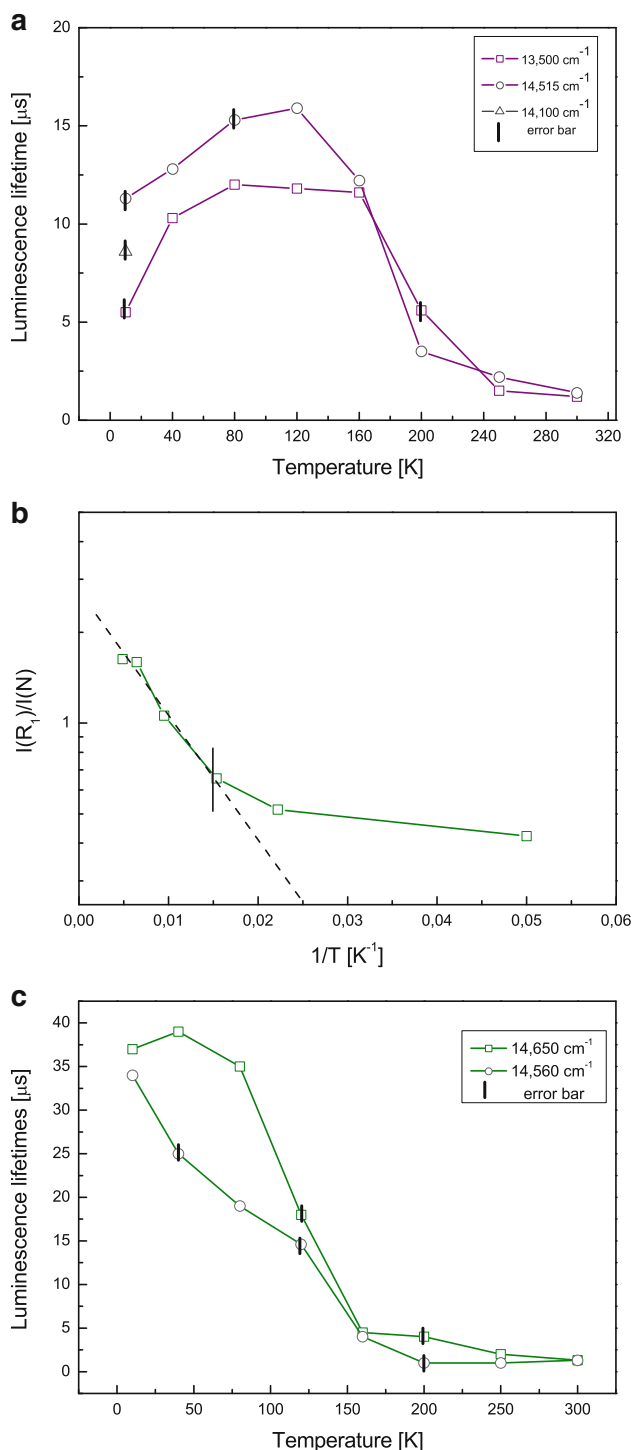
**a**



**b**



**c**



**Fig. 5 a** The temperature dependence of the luminescence lifetime of three distinct emission lines of the $Cr^{3+}$ ion in *purple chlorite*. **b** The temperature dependence of the relative luminescence intensities of the $R_1$ and N line in *green chlorite*. **c** The temperature dependence of the luminescence lifetime of two distinct emission lines of the $Cr^{3+}$ ion in *green chlorite*

(d)   its fluorescence lifetimes and those of $R_1$ are comparable and change similarly with temperature (Fig. 5c);

(e)   the additional emission line at 14,560 $cm^{-1}$ cannot be attributed to non-equivalent $Cr^{3+}$ centers like for topaz (Tarashchan et al.2006) or spodumene crystals (Walker et al.1997) because of their much lower Cr content compared to chlorite crystals, and because of different luminescence properties at low temperature.

In contrast to the Powell et al. results, the luminescence lifetimes of emissions from single $Cr^{3+}$ and from Cr–Cr pairs are very short and distinctly shrinking already for the initial growth of temperature (Fig. 5c). The energy transfer to other luminescence centers, primarily to $Fe^{2+}$ ions, must be the basic factor causing such a short lifetime for the $R_1$ line. The luminescence decay is single exponential; thus, the energy transfer has mainly a resonance character.

## Conclusions

1. Chromium ions are present in the M4 crystal site (brucite sheet) in the purple chlorite, but in the green chlorite, they occupy the M1 or M2 site in the inner octahedral sheet. The $Cr^{3+}$—ligand bond reveals a rather ionic character in the green chlorite and an ionic-covalent character in the purple chlorite. The differences in the Dq and B parameters of these two chlorite crystals are caused not only by differences in metal–ligand distances, but also by differences in the effective negative charge on ligands as well as of the effective positive charge on the $Cr^{3+}$ cation.

2. The high $Cr_2O_3$ content in both crystals does not completely quench the luminescence, and concentration quenching of the luminescence is observable in this case. Emission from the Cr-cluster as well as from $Cr^{3+}$ ions adjacent to cationic vacancies in the brucite sheet is demonstrated for the purple chlorite crystal; for the green chlorite, the emission from the N pair has been observed.

3. It is generally difficult to identify the dominant type of quenching centers in the studied chlorite crystals. The quenching is enhanced through energy migration to perturbed Cr sites or to impurities than can dissipate the energy without radiation. High Cr content and energy transfer from all $Cr^{3+}$-emission centers to $Fe^{2+}$ ions are regarded as the main causes of the luminescence lifetime reduction.

4. The content of $Fe^{3+}$ ions in tetrahedral coordination is higher for the green chlorite than for the purple, and the preference of the M2 site by $Fe^{2+}$ is distinctly higher for the green chlorite than it is for the purple. The M1 and M2 sites in the purple Cr-clinochlore seem to be more regular than in the green specimen.

5. For the green chlorite, higher numbers of $Al^{3+}$ ions in the tetrahedral sheet and heavy atoms in the inner octahedral sheet have been observed than for the purple chlorite.

# References

Andrut M, Wildner M, Taran M, Langer K, Schulz R (1995) Temperature dependent polarized single crystal absorption spectra of kaemmererite. Phys Chem Miner 23:242–243

Annersten H (1974) Mössbauer studies of natural biotites. Am Mineral 59:143–151

Bailey SW (1975) Chlorites. In: Giesing JE (ed) Soil components, vol 2. Springer, New York, pp 191–263

Bailey SW, Brown BE (1962) Chlorite polytypism. I. Regular and semi-random one-layer structures. Am Mineral 47:819–850

Barthem RB, Abritta Y, Eichler JPF, DeSoura Barro F (1982) Some properties of the fluorescence spectra of heavily doped ruby. J Lumin 27:213–235

Bish DL (1977) An spectroscopic and X-ray study of the coordination of $Cr^{3+}$ ions in chlorites. Am Mineral 62:385–389

Blaauw C, Stroink G, Leiper W (1980) Mössbauer analysis of talc and chlorite. J Physique 41:C1-411–C1-412

Brown BE, Bailey SW (1963) Chlorite polytypism II: crystal structure of a one-layer Cr-chlorite. Am Mineral 48:42–61

Czaja M (1999) Excited states of transition elements. Duszniki Zdrój, Poland, Abstract, Polish Academy of Science P09

Czaja M (2002) Luminescencja jonów chromu w naturalnych krzemianach. In Polish. Wydawnictwo Uniwersytetu Śląskiego Katowice

DeGrave E, Vandenbruvaene J, van Bockstael M (1987) $^{57}Fe$ Mössbauer spectroscopic analysis of chlorite. Phys Chem Minerals 15:173–180

Dereń PJ, Malinowski M, Stręk W (1996) Site selection spectroscopy of $Cr^{3+}$ in $MgAl_2O_4$ green spinel. J Lumin 68:91–103

Dyar MD (1987) A review on Mössbauer data on trioctahedral micas: evidence for tetrahedral $Fe^{3+}$ and cation ordering. Am Mineral 72:102–112

Dyar MD, Agresti DG, Schaefer MW, Grant CA, Sklute EC (2006) Mössbauer spectroscopy of earth and planetary materials. Annu Rev Earth Planet Sci 34:83–125

Farmer VC (1974) The layer silicate. In: Farmer VC (ed) The infrared spectra of minerals. Miner Soc Monograph 4, London, pp 331–363

Foster MD (1962) Interpretation of the composition and a classification of the chlorites. U.S. Geol Survey Prof paper 414-A

Gaft M, Nagli L, Reisfeld R, Panczer G, Brestel M (2003) Time-resolved luminescence of Cr3+ in topaz Al2SiO4(OH, F)2. J Lumin 102–103:349–356

Goodman BA, Bain DC (1979) Mössbauer spectra of chlorites and their decomposition products. Dev Sedymentol 27:65–74

Gregori DA, Mercader RC (1994) Mössbauer study of some Argentinian chlorites. Hyperfine Interact 83:495–498

Illaremandi MA, Balda R, Fernandez J (1993) Antiresonance in the excitation and absorption spectra of $Cr^{3+}$-doped fluoride glasses. Phys Rev B 47:8411–8417

Imbush GF (1967) Energy transfer in ruby. Phys Rev 133:326–337

Lister JS, Bailey SW (1967) Chlorite polytypism IV: regular two-layer structures. Am Miner 52:1614–1631

Morata D, Higueras P, Dominguez-Bella S, Parras J, Velasco F, Aparicio P (2001) Fuchsite and other Cr-rich phyllosilicates in ultramafic enclaves from Almaden mercury mining district, Spain. Clay Miner 36:345–354

Phillips TL, Loveless JK, Bailey SW (1980) $Cr^{3+}$ coordination in chlorites: a structural study of ten chromian chlorites. Am Mineral 65:112–122

Płatonow AN, Langer K, Calas G, Andrut M (1995) Optical absorption spectroscopy of $Cr^{3+}$-ions in phyllosilicates. Phys Chem Miner 23(241):242

Powell RC, DiBartolo B, Birang B, Naiman CS (1967) Fluorescence studies of energy transfer between single and pair $Cr^{3+}$ systems in $Al_2O_3$. Phys Rev 155:296–308

Prieto AC, Dubessy J, Cathelineau M (1991) Structure-compositional relationships in trioctahedral chlorites: a vibrational spectroscopy study. Clays Clay Miner 39:531–539

Prieto AC, Boiron M-C, Cathelineau M, Mosser-Ruck R, Lopez JA, García C (2003) Rythmic changes in crystal chemistry of trioctahedral Cr-chlorites and Cr-entrapment: a SEM, EM and Raman study. Clay Miner 38:339–352

Scholtzová E, Tunega D, Turi Nagy DJ (2003) Theoretical study of cation substitution in trioctahedral sheet of phyllosilicates. An effect of inner OH group. J Mol Struct 620:1–8

Shirozu H (1980) Cation distribution, sheet thickness, and O–OH space in in trioctahedral chlorites—An X-ray and infrared study. Miner J 10:14–34

Shirozu H (1985) Infrared spectra of trioctahedral chlorites in relation to chemical composition. Clay Sci 6:167–176

Shirozu H, Ishida K (1982) Infrared spectra of 7 Å and 14 Å layers. Miner J 11:161–171

Smyth JR, Darby Dyar M, May HM, Bricker OP, Acker JG (1997) Crystal structure refinement and m össbauer spectroscopy of an ordered triclinic clonochlore. Clays Clay Miner 45:544–550

Steinfink H (1958) The crystal structure of chlorite. II. A triclinic polymorph. Acta Cryst 11:191–195

Stręk W, Łukowiak E, Jeżowska-Trzebiatowska B (1983) Observation of antiresonance in fluorescence spectra of $Cr^{3+}$ and $Nd^{3+}$ doped glasses. A Naturforsch 38a:587–588

Stubican V, Roy R (1961) Isomorphous substitution and infrared spectra of the layer lattice silicates. Am Mineral 46:32–51

Szymczak H, Wardzyńska M, Myknikova IE (1975) Optical spectrum of $Cr^{3+}$ in the spinel $LiGa_5O_8$. J Phys C 8:3937–3943

Tarashchan AN, Taran MN, Rager H, Iwanuch W (2006) Luminescence spectroscopy study of $Cr^{3+}$ in Brazilian topazes from Ouro Preto. Phys Chem Minerals 32:679–690

Tuddenham WM, Lyon RPJ (1959) Relation of infrared spectra and chemical analysis of some chlorites and related minerals. Anal Chem 31:377–380

Walker G, ElJaer A, Sherlock R, Glynn TJ, Czaja M, Mazurak Z (1997) Luminescence spectroscopy of $Cr^{3+}$ and $Mn^{2+}$ in spodumene ($LiAlSi_2O_6$). J Lumin 72–74:278–280

Zheng H, Bailey SW (1989) Structures of intergrown triclinic and monoclinic II*b* chlorites from Kenya. Clays Clay Miner 37(308):316